Journal of Gerontology: BIOLOGICAL SCIENCES
2007, Vol. 62A, No. 3, 235–245

Accumulation of Mitochondrial DNA Deletion Mutations in Aged Muscle Fibers: Evidence for a Causal Role in Muscle Fiber Loss

Allen Herbst, Jeong W. Pak, Debbie McKenzie, Entela Bua, Marwa Bassiouni, and Judd M. Aiken

Department of Animal Health and Biomedical Sciences, University of Wisconsin, Madison.

Although mitochondrial mutation abundance has been recognized to increase in an age-dependent manner, the impact of mutation has been more difficult to establish. Using quantitative polymerase chain reaction, we measured the intracellular abundance of mutant and wild-type mitochondrial genomes along the length of individual laser-captured microdissected muscle fibers from aged rat quadriceps. Aged muscle fibers possessed segmental, clonal intracellular expansions of unique somatically derived mitochondrial DNA (mtDNA) deletion mutations. When the mutation abundance surpassed 90% of the total mitochondrial genomes, the fiber lost cytochrome *c* oxidase activity and exhibited an increase in succinate dehydrogenase activity. In addition to the mitochondrial enzymatic abnormalities, some fibers displayed abnormal morphology such as fiber splitting, atrophy, and breakage. Deletion mutation accumulation was linked to these aberrant morphologies with more severe cellular pathologies resulting from higher deletion mutation abundance. In summary, our measurements indicate that age-induced mtDNA deletion mutations expand within individual muscle fibers, eliciting fiber dysfunction and breakage.

DUE to a multifactorial etiology, the specific series of molecular events that contribute to the aging process has not been elucidated. Dissecting and deciphering specific physiological mechanisms responsible for age-associated phenotypes is critical for advancing our understanding of the aging process. In accordance with the mitochondrial theory of aging (1,2), the accumulation of defective mitochondrial genomes has contributed to the physiological decline associated with aging (3–5). Sarcopenia, the age-associated loss of skeletal muscle mass and function (6), is a prime nonpathological contributor to the frailty associated with aging. Of the proposed mechanisms for sarcopenia (loss of muscle stem cell activity, denervation and/or renervation, endocrine changes, oxidative stress, or mitochondrial genome instability), the cumulative loss of individual muscle fibers represents a primary and permanent deficit.

In humans, 40% of muscle mass is lost between the ages of 20 and 80 (7). This muscle mass loss is due to decreased muscle cross-sectional area, loss of muscle fibers, and fiber atrophy (8,9). In the rat quadriceps muscles, rectus femoris and vastus lateralis, muscle mass decreased by 33% and 60% and fiber number decreased 30% and 58% between 18 and 36 months of age (10,11).

Concurrent with the age-dependent loss of muscle fibers, multiple mitochondrial DNA (mtDNA) deletion mutations accumulate over time in many tissues and species (12–16). MtDNA deletion mutations were initially considered to be at low abundance ($<0.1\%$) when calculated against the total mitochondria pool in tissue homogenates (17,18). When, however, discrete numbers of muscle fibers were analyzed, the abundance of mtDNA deletion mutations was found to be inversely proportional to the number of cells analyzed (19). In situ hybridization studies demonstrated that mtDNA deletion mutations were not distributed homogeneously throughout a tissue, but amplified focally within a subset of individual cells, appearing as a segmental pattern along the length of muscle fibers and as a mosaic distribution between cells (20–26).

Mammalian mitochondria encode 22 transfer RNAs (tRNAs), 2 ribosomal RNAs (rRNAs), and 13 polypeptides from a 16.5-kilobase circular genome. Mitochondrial genomes exist as a cellular multiplicity and, as a result, mtDNA molecules complement each other, protecting against deleterious mutations. When mutations do occur, a state of heteroplasmy exists within individual mitochondria and cells. The cellular and systemic impact of mtDNA mutation is illustrated by a group of genetic diseases known as the mitochondrial myopathies and encephalomyopathies (27–29). Mitochondrial diseases are caused by the intracellular accumulation of mutated mtDNA to levels that eventually disrupt the synthesis of mitochondrially encoded components of the electron transport system (ETS). The abundance at which specific mutations cause ETS dysfunction is termed the phenotypic threshold effect (reviewed in 30,31). A characteristic cellular phenotype exhibited by patients with mitochondrial myopathies is the histological absence of cytochrome *c* oxidase (COX) activity and an upregulation of succinate dehydrogenase (SDH) activity (24). In situ hybridization studies on COX^{-} fibers measured mitochondrial transcript abundance and/or mtDNA concentrations and

Table 1. Primers for Quantitative Polymerase Chain Reaction

Fiber	Primer Pair	Wt/del	Sequence 5′-3′
1,2,4	RM13645F	Wt	CAACATAACCCCAACATCATCAATCTCATACA
	RM13927R		AATAGTTTTAGGGTTTGGGGGTTCGTTTTT
1	RM7290F	del	AGGACACCAATGATACTGAAGCTATGAATATACTGACTA
	RM14786R		ATGGAATGGGATTTTGTCTGCGTCG
2	RM5981F	del	CTTCGACCCCGCTGGAGGTGGAGAC
	RM14347R		GATGAGAATGCTGTTATGGTATCAGACGTGTAGTG
3	RM7189F	Wt	ATTCTCCCAGCTGTCATTCTTATTCTAATTGCCCTTCC
	RM7332R		TTCATAGTCAGTATATTCATATTCATAGCTTCAGTATCATTGGTGTCCT
3	RM5360F	del	CCTCTATAGGCTCATTCATCTCACTTACGCC
	RM12683R		GCAAATGTGGAGGAAAGCAAGGTAGGGT
4	RM7347F	del	CTCCTACATAATCCCAACCAATGACCTAAAACC
	RM14675R		GATGAAGTGGAATGCGAAGAAGCGTGT

Note: Wt = Wild-type specific primer; del = deletion specific primers.

found that wild-type and deletion-specific transcript levels were proportional to genotype abundance (20–23). Some studies found that wild-type genomes were reduced, whereas others suggested that wild type was maintained in COX^{-} regions [reviewed by Shoubridge (32)].

Whereas the same mtDNA mutation is distributed among multiple tissues in the mitochondrial myopathies and encephalomyopathies, mitochondrial mutations also originate as a result of spontaneous somatic mutation events within individual cells. These age-associated mtDNA deletion mutations also induce COX^{-}/SDH^{++} fibers, and are distributed mosaically intercellularly and segmentally intracellularly (26). Thus, accurate quantitation of the abundance of these enzymatic abnormalities requires the analysis of numerous sections of tissue along the length of the muscle. Based on histological analysis of aged muscles, the calculated tissue burden of ETS abnormalities was found to be 15% of all remaining muscle fibers in 36-month old rat rectus femoris (10), and 60% in 34-year-old rhesus monkey vastus lateralis (26). Additionally, muscles that display a large age-dependent loss of skeletal muscle fibers contain high levels of ETS abnormalities (33). Concomitant with observed ETS enzymatic abnormalities are often morphological changes in muscle fiber structure including fiber splitting, atrophy, and breakage.

The association of ETS abnormalities, mtDNA deletion mutations, fiber loss, and muscle mass loss suggest that these age-dependant events might share a common etiology. In this study, we tested the hypothesis that mtDNA mutation accumulation underlies the fiber splitting, atrophy, and breakage associated with ETS abnormalities. By taking a longitudinal single fiber approach to understanding the relationship between mitochondrial genotype and cellular phenotype, we link mtDNA deletion mutation accumulation with these dysfunctional cellular phenotypes and, ultimately, with muscle fiber loss.

Methods

Animals and Tissue Preparation

The rectus femoris and the vastus lateralis muscles were dissected from 36-month-old male Fischer 344 × Brown Norway F1 hybrid rats purchased from the National Institute on Aging colony maintained by Harlan Sprague Dawley (Indianapolis, IN). Rats were housed and killed in accordance with the Guide for the Care and Use of Laboratory Animals. The muscles were bisected at the midbelly, embedded in optimal cutting temperature medium (Miles Inc., Elkhart, IN), and flash frozen in liquid nitrogen. Samples were stored at –80°C until analyzed. Using a cryostat, we cut 100 or 200 10-μm-thick serial transverse cryosections and placed them on Probe-on Plus slides. At 60 μm intervals, cross-sections were stained for COX and SDH as previously described (10), and ETS abnormal fibers were identified. Fibers were also stained for cell morphology and nuclei with hematoxylin and eosin.

Laser Capture Microdissection

Histological sections were dehydrated through a series of graded ethanol and xylene (10). ETS abnormal fibers were subsequently microdissected using a PixCell II laser capture microscope (Arcturus, Mountain View, CA). Finally, captured fibers were further dissected from the capture film to eliminate all potential contamination.

DNA Isolation, Breakpoint Analysis, and Quantitative Real-Time Polymerase Chain Reaction

DNA isolation and mtDNA breakpoint analysis were performed as previously described (34). Oligonucleotide primers (Table 1) specific for either full-length or deleted genomes were designed for use in quantitative polymerase chain reaction (PCR) assays based on the unique sequence of each mtDNA deletion obtained from the breakpoint analysis. The full-length primer set is designed to amplify a region of the genome within the confines of the deleted mtDNA, ensuring the s specific amplification of full-length wild-type genomes. Deletion primer sets flank the breakpoint such that amplification of the deleted genomes yields an amplicon of ~200 base pairs. The deletion primer sets cannot amplify full-length mtDNA due to the short extension time in the elongation phase of the PCR. Total DNA concentration is determined every cycle by the fluorescence emission generated by the binding of SYBR Green to the minor groove of DNA. Microdissected samples are amplified in parallel with known standards generated by cloning the deletion-specific as well as full-length sequences into the

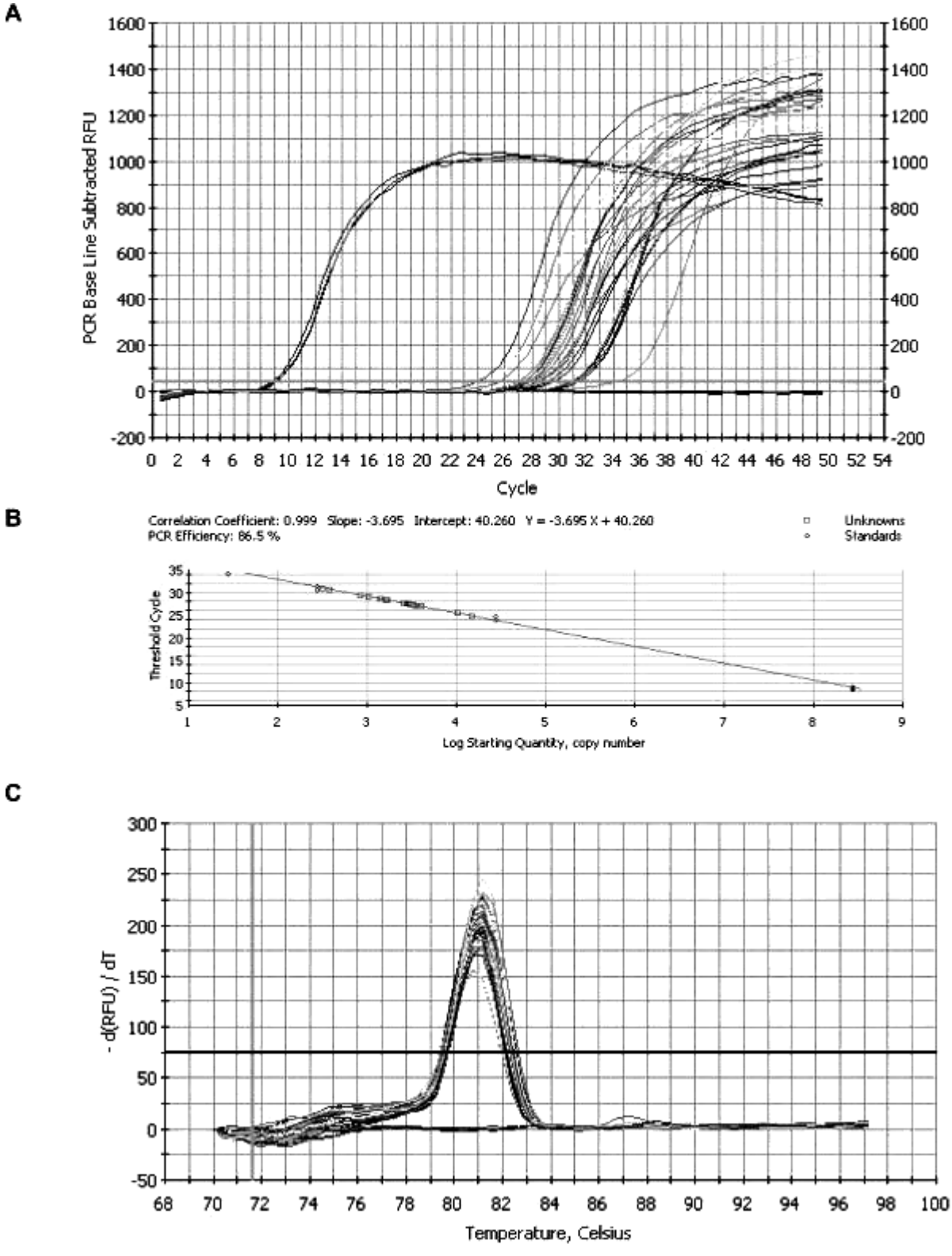

Figure 1. Typical quantitative polymerase chain reaction data from wild-type primer pair RM13645F–RM13927R. (**A**) Amplification curves for standards and mitochondrial DNA (mtDNA) from laser-captured muscle fibers. Baseline curves are no-template control reactions. RFU = Relative fluorescence units. (**B**) Standard curve generated by amplifying cloned wild-type standards. Log starting quantity of the mtDNA from the laser-captured sample is interpolated from the equation of the best-fit line. (**C**) Melt-curve analysis of real-time amplification products illustrating the specificity of melting temperature and confirming product identity. Plot of the first derivative of fluorescence with regard to temperature.

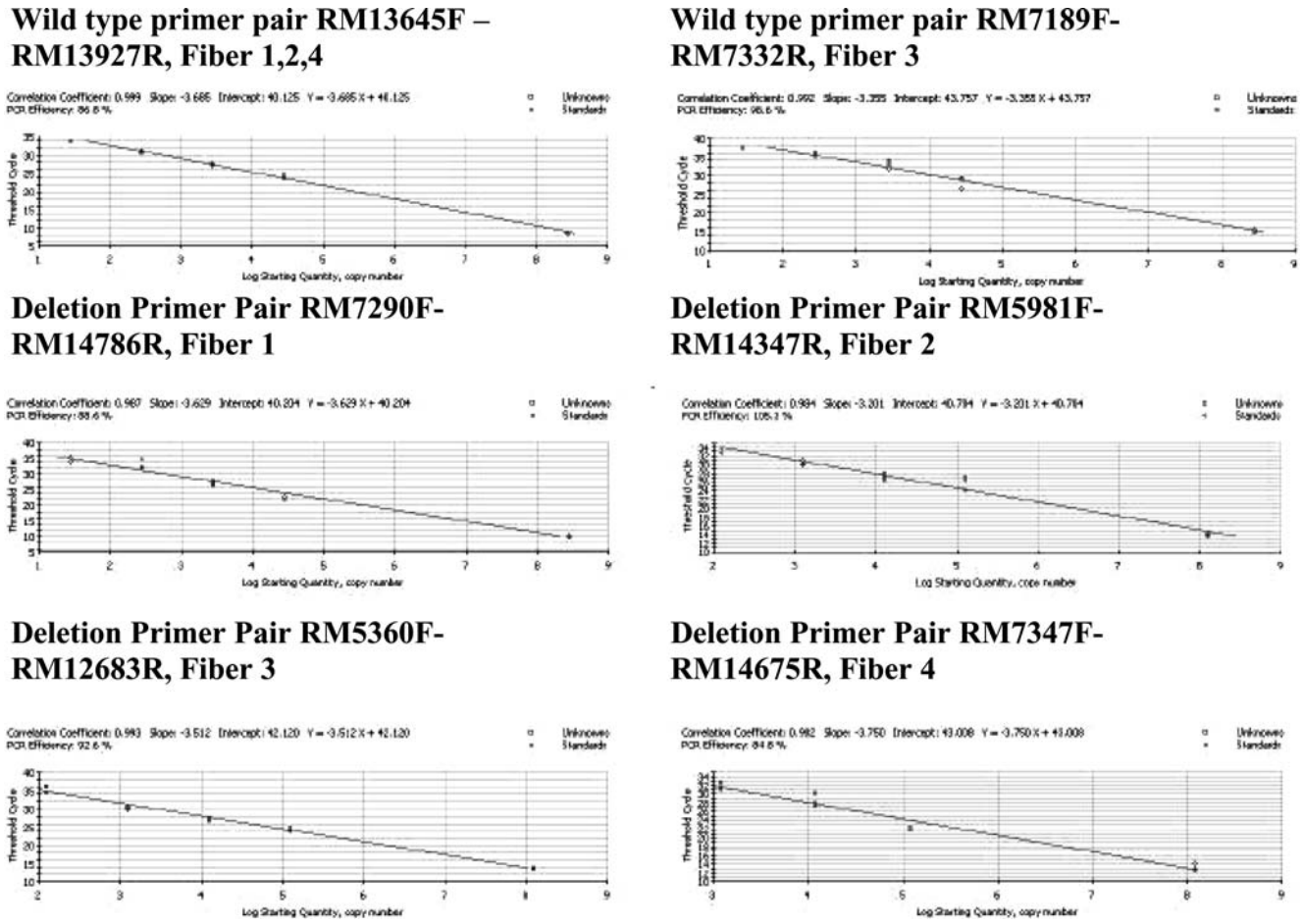

Figure 2. Standard curves generated by amplifying serial dilutions of wild-type or deletion-specific plasmids.

pGEM T-easy vector (Promega, Madison, WI). Standards were quantified by spectrophotometry at A_{260}, and dilutions were prepared using National Institute of Standards and Technology (NIST)–calibrated volumetric pipets. Linearity of dilutions was confirmed by quantitative PCR and regression analysis. Samples and standards for both wild-type and deletion-specific primer sets were amplified in triplicate using iQ SYBR Green supermix (BIO-RAD Laboratories, Hercules, CA). Standard curves were generated for the primer sets (Figures 1B and 2), and the starting quantities of wild-type and deleted mitochondrial genomes were calculated. Specificity of amplification reactions was confirmed by melting point analysis (Figure 1C) and gel electrophoresis.

Results

Serial longitudinal cross-sections of aged muscle tissue were stained histochemically at 60 μm intervals to identify muscle fibers containing ETS abnormal regions (Figures 3–6A). Four fibers containing COX^{-}/SDH^{++} regions were selected based on their morphology and the contiguity of the ETS abnormal region within the series of sections. Fibers 1 and 2 contain a 440 μm and 460 μm nonatrophic ETS abnormal phenotype (Figures 3 and 4). Fiber 3 contains an ETS abnormal region that colocalizes with a region undergoing fiber splitting. The fiber splits along its length first into two and, subsequently, three fibers before returning to a single unified fiber (Figure 5). Fiber 4 atrophies, eventually becoming undetectable for 250 μm, and then reappears as an ETS abnormal fiber (Figure 6).

Multiple sections of each of these fibers were individually microdissected, DNA-isolated and, through the use of mtDNA-specific primers, amplified and subsequently sequenced. A single smaller-than-wild-type genome (an mtDNA deletion mutation) was identified in each fiber's ETS abnormal region. The size of these deletion-containing genomes varied between fibers and ranged from 8148 to 11,268 base pairs. All deletion mutations removed portions of the wild-type mitochondrial genome along the major arc and disrupted or abrogated genes coding for COX, ATP synthase, NADH dehydrogenase, as well as the interspersed mitochondrial tRNAs. The specific deletion mutation in fiber one removed nucleotides 6013–14,165, fiber two nucleotides 7455–14,731, fiber three nucleotides 6710–12,542 and fiber four nucleotides 7389–14,485.

The absolute quantity of deleted and wild-type mitochondrial genomes was determined by breakpoint-specific

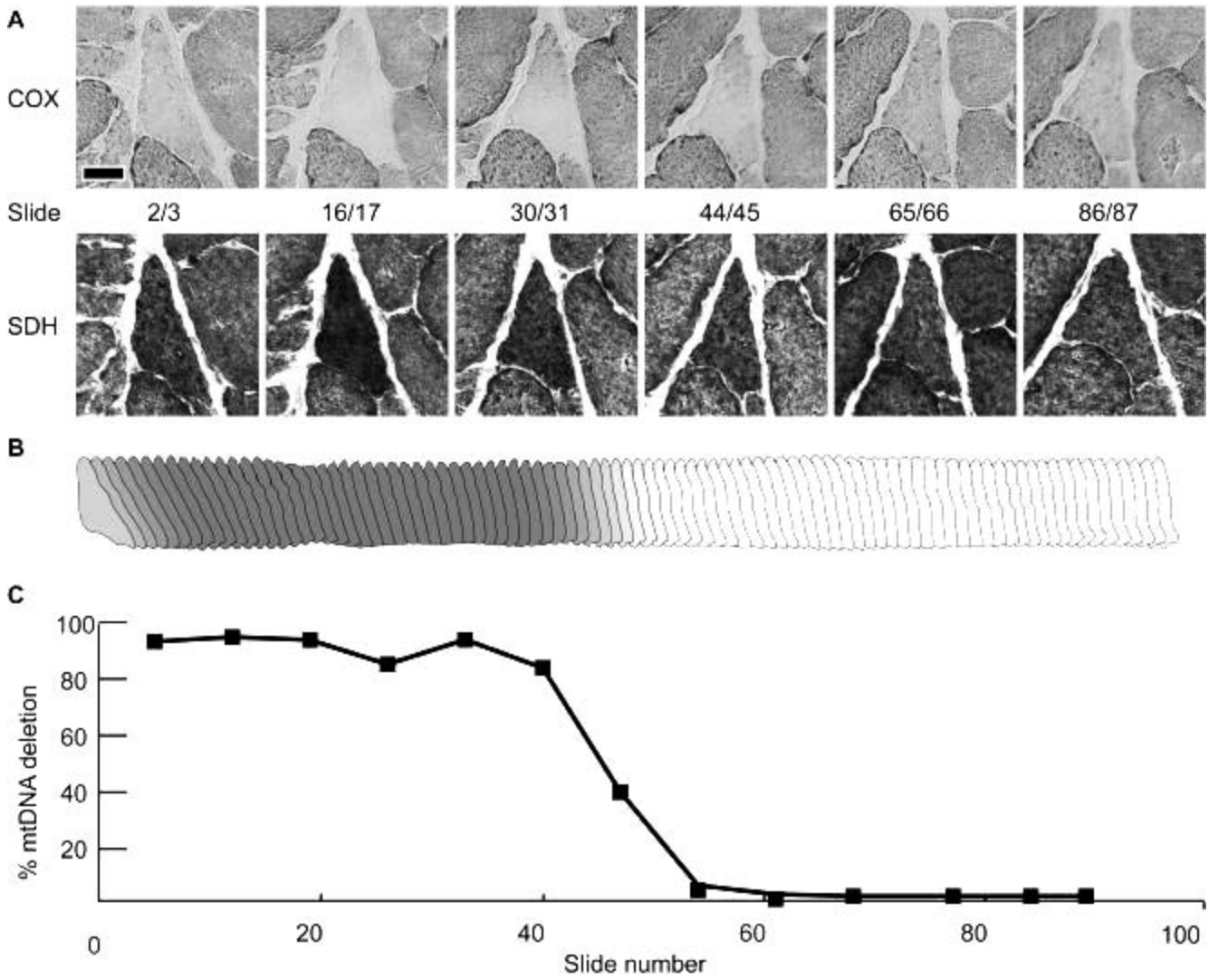

Figure 3. *Fiber 1*. (**A**) Serial micrographs showing enzymatic staining for cytochrome *c* oxygenase (COX) and succinate dehydrogenase (SDH). Scale bar = 25 μm. (**B**) Morphometric digital reconstruction of fiber 1. The intensity of the shaded area denotes the severity of the electron transport system abnormal phenotype. (**C**) Percentage of mitochondrial DNA (mtDNA) genomes that are mutant along the length of the abnormal fiber.

quantitative PCR assays on laser-captured cell sections collected along the length of individual muscle fibers. The intracellular abundance of mtDNA deletion mutations within each fiber's ETS abnormal region was greater than 90%. In every fiber, the COX^{-}/SDH^{++} phenotype was flanked by adjacent ETS normal regions that contained detectable levels of deletion mutations, albeit at lower levels (Figures 3–6). Fiber 1, for example, contained a 440-μm ETS abnormal region within a 770-μm region that contained an accumulation of mtDNA deletion mutations. As the abundance of mtDNA mutation decreased, there was an intermediate ETS abnormal transitional phenotype characterized by slightly reduced COX activity, and slightly increased SDH activity (Figures 3A [slides 44/45] and 4A [slides 16/17]). In fiber regions distant from the ETS abnormality, only wild-type genomes were detected, and mtDNA deletion mutations were undetectable. The COX-negative, SDH hyper phenotype occurred in regions that contained greater than 90% mutant mtDNA (Figures 3–6). Wild-type genomes were consistently detected in both ETS normal and abnormal regions (Figure 7).

Discussion

Age-associated mtDNA deletion mutations form as the result of somatic mutation of wild-type genomes. The cellular impact, however, is the result of the clonal accumulation of mutant genomes to sufficiently high levels to affect mitochondrial and cellular function. The presence of mutant mtDNA genomes outside the ETS abnormal phenotype (Figures 3–6) indicates that the ETS abnormal phenotype results from the intracellular accumulation of mtDNA deletion mutations, not vice versa. The maintenance of wild-type genomes throughout the abnormal region (Figure 7) at levels that are similar to ETS normal regions and the coordinated decrease in mutation abundance in the

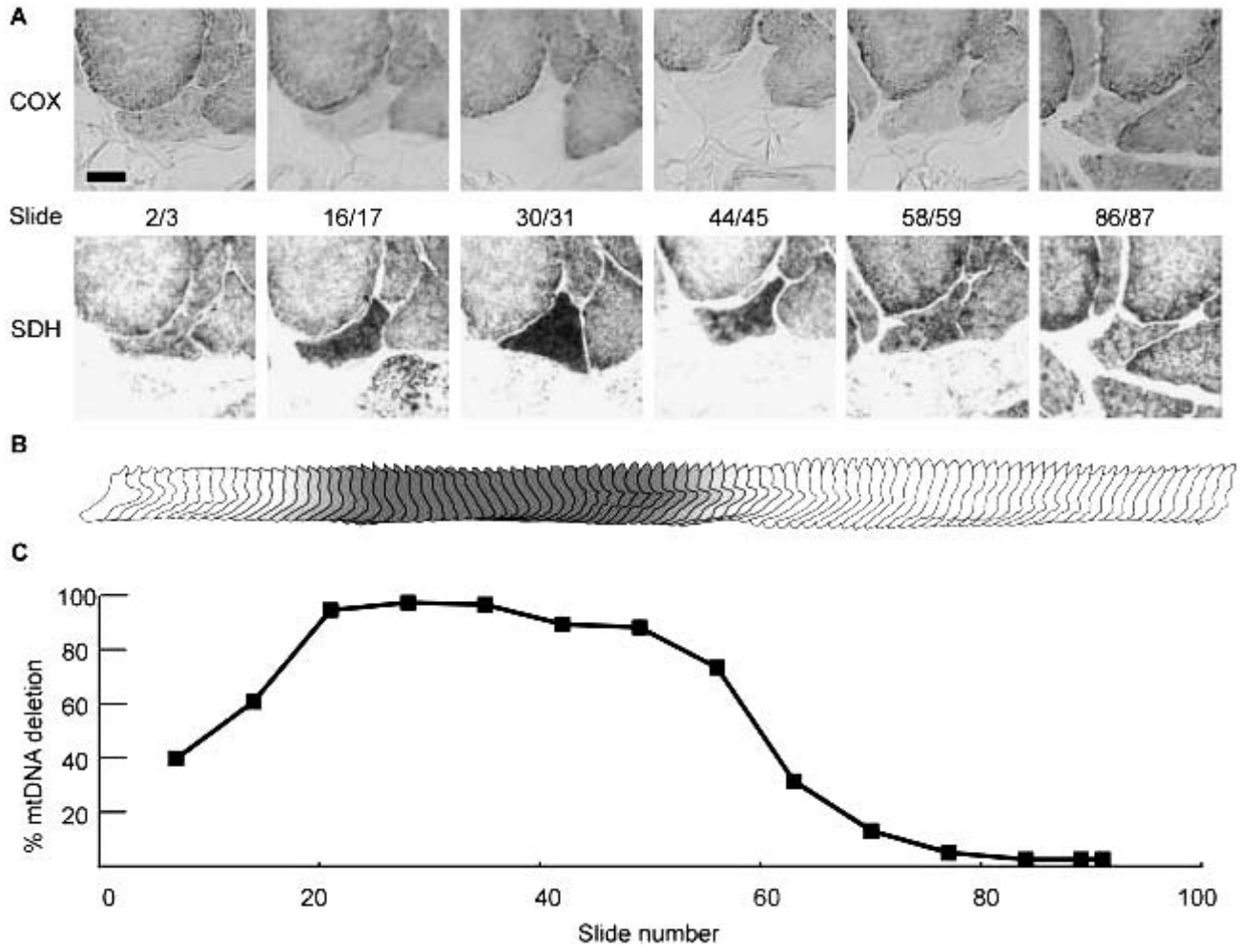

Figure 4. *Fiber 2*. (**A**) Serial micrographs showing enzymatic staining for cytochrome *c* oxygenase (COX) and succinate dehydrogenase (SDH). Scale bar = 25 μm. (**B**) Morphometric digital reconstruction of fiber 2. The intensity of the shaded area denotes the severity of the electron transport system abnormal phenotype. (**C**) Percentage of mitochondrial DNA (mtDNA) genomes that are mutant along the length of the abnormal fiber.

ETS normal region indicate that the accumulation of deleted genomes, and not the selective depletion of wild type, is responsible for phenotypic threshold effect. The loss of COX activity in the presence of wild-type genomes suggests that incompetent genomes and their derived transcripts may compete with wild-type genomes for binding of transcriptional and translational machinery leading to a breakdown in the amount of functional polypeptides and loss of enzymatic activity.

We measured the absolute quantity of mitochondrial genomes, full-length and deletion-containing, to determine the threshold for the loss of COX activity. A 90% threshold for age-induced mtDNA mutations is consistent with previous measurements that determined the threshold for loss of COX activity to be between 60% (35) and 90% (20,21,36), depending upon tissue type (HeLa cells, or multinucleated muscle fibers from patients with mitochondrial myopathies, respectively). The maintenance of full-length wild-type genomes in ETS abnormal segments is consistent with in situ hybridization studies from patients with mitochondrial myopathies (20,21) as well as aged muscle fibers (25,26).

Muscle fiber splitting is a characteristic phenotype of many primary muscle diseases including dystrophies. In the split muscle fiber (Figure 5), the same molecular mutation was detected in each of the daughter fibers, indicating that the mutation was present before the split occurred and, consequently, that the fiber is undergoing splitting and not fusion. Muscle fiber splitting has been observed to be associated with 35% of ETS abnormal muscle fibers; however, the split region rarely colocalized with the abnormal enzymatic phenotype (10). Our data suggest that, whereas there is no overlap between the ETS abnormal region and the split fiber regions, there is a colocalization of fiber splitting and the accumulation of mtDNA deletion mutations (Figure 5C), albeit at levels below the threshold for the expression of the ETS abnormal phenotype. Splitting may represent a precursor phenotype to fiber atrophy via the independent breakage of daughter fibers or a protective mechanism that allows segregation of mutant and

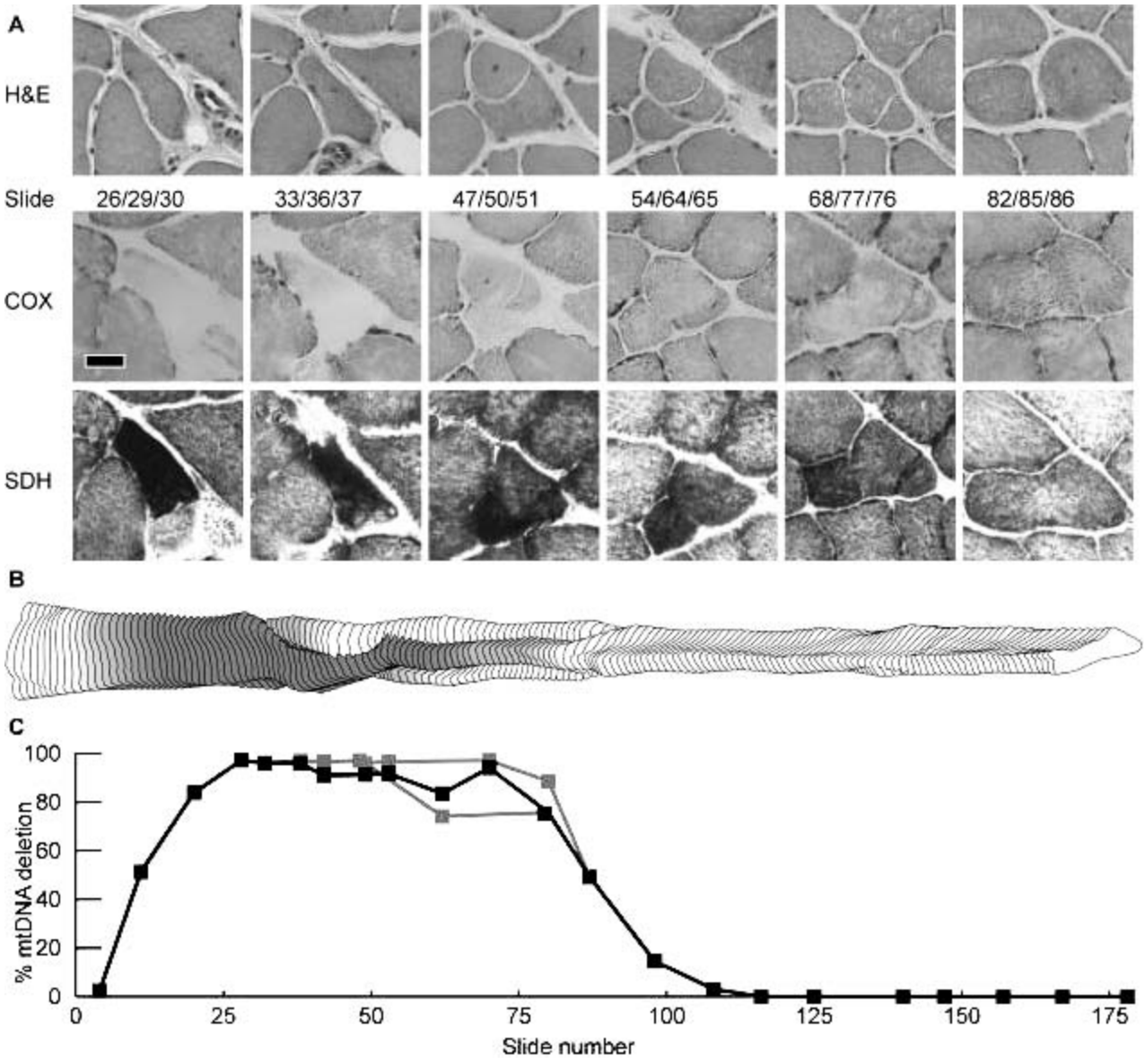

Figure 5. *Fiber 3*. (**A**) Serial micrographs staining for morphology with hematoxylin and eosin (H&E) and enzymatic activities for cytochrome *c* oxygenase (COX) and succinate dehydrogenase (SDH). The muscle fiber splits into three distinct subfibers before fusing back together. The deletion mutation was detected throughout 1080 μm. Scale bar = 25 μm. (**B**) Morphometric digital reconstruction of fiber 3. The intensity of the shaded area denotes the severity of the electron transport system abnormal phenotype. (**C**) Percentage of mitochondrial DNA (mtDNA) genomes that are mutant along the length of the abnormal fiber. The unique mtDNA deletion mutation was found at high levels within different branches of the same fiber.

wild-type genomes altering the level of heteroplasmy in each branch.

We have previously reported, in aged rat quadriceps muscle, that 25% of ETS abnormal fibers are associated with fiber atrophy and 7% with fiber breakage (10). Similar observations have been made in rhesus macaques (25,26). The proliferation of an mtDNA deletion mutation across a broken fiber segment (Figure 6) and the subsequent ETS abnormality directly supports the hypothesis that accumulation of mtDNA deletions can result in fiber breakage. The broken ends of the fiber (Figure 6C) contain exceedingly high levels of the same unique mtDNA deletion mutation suggesting that the fiber was once continuous, subsequently atrophied, and ruptured. The broken ends of the fiber contain the highest level of mtDNA mutations measured, 3×10^5 mutant genomes, demonstrating a profound ETS abnormal phenotype.

The mechanism driving mtDNA deletion mutation proliferation is not known. MtDNA deletion mutations could accumulate because they possess a replication advantage, because of stochastic events, or because their destruction is disadvantaged. These possibilities have been put forth as biological hypotheses: replicative advantage (21), random drift (37), and survival of the slowest (38), respectively.

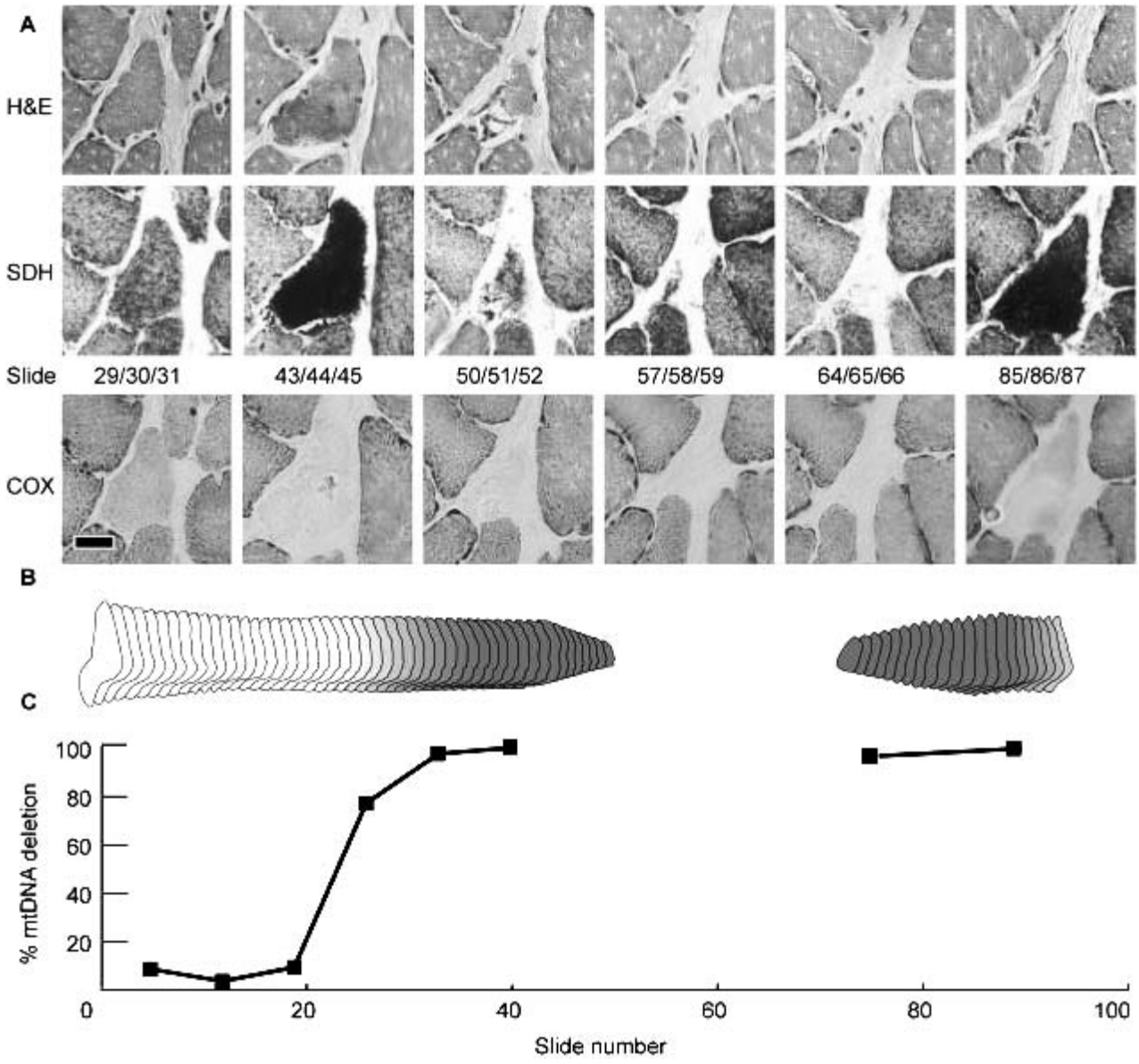

Figure 6. *Fiber 4*. (**A**) Serial micrographs staining for morphology with hematoxylin and eosin (H&E) and enzymatic activities for cytochrome *c* oxygenase (COX) and succinate dehydrogenase (SDH). The electron transport system abnormal region extends for over 700 μm and includes a 250 μm region where the fiber has ruptured and cannot be detected. Scale bar = 25 μm. (**B**) Morphometric digital reconstruction of fiber 4. The intensity of the shaded area denotes the severity of the ETS abnormal phenotype. (**C**) Percentage of mitochondrial DNA (mtDNA) genomes that are mutant along the length of the abnormal fiber. The same mtDNA deletion mutation is detected across the broken fiber region, and the highest levels (>99%) of mutation are found immediately flanking the fiber break.

These mechanisms are not mutually exclusive, however, and the mechanism of mtDNA accumulation may be more complex, especially in multinucleated tissue such as muscle fibers. The strikingly high copy number of deletion-containing genomes (~100,000 copies) measured within an ETS abnormal section, combined with the relatively stable numbers of wild-type genomes (~1000 copies), implies that muscle fibers do not maintain a steady state of mtDNA molecules in response to dysfunctional oxidative phosphorylation. That is, mitochondrial deletion mutation replication does not occur at the expense of wild-type replication. Moreover, these measurements suggest that deleted mtDNA molecules are advantaged, replicating to high abundance. One prediction of the advantaged model is the presence of neutral mtDNA deletion mutations that do not accumulate to high levels due to genome size or specific breakpoint location. We compared the specific deletion mutation breakpoints that accumulate in individual ETS abnormal fibers with the breakpoint sequences observed in muscle tissue homogenates (Figure 8). The deletion breakpoints in tissue homogenates were distributed throughout the mitochondrial genome, whereas deletion breakpoints from abnormal fibers were confined to the major arc of the mtDNA indicating specificity for mutations that could

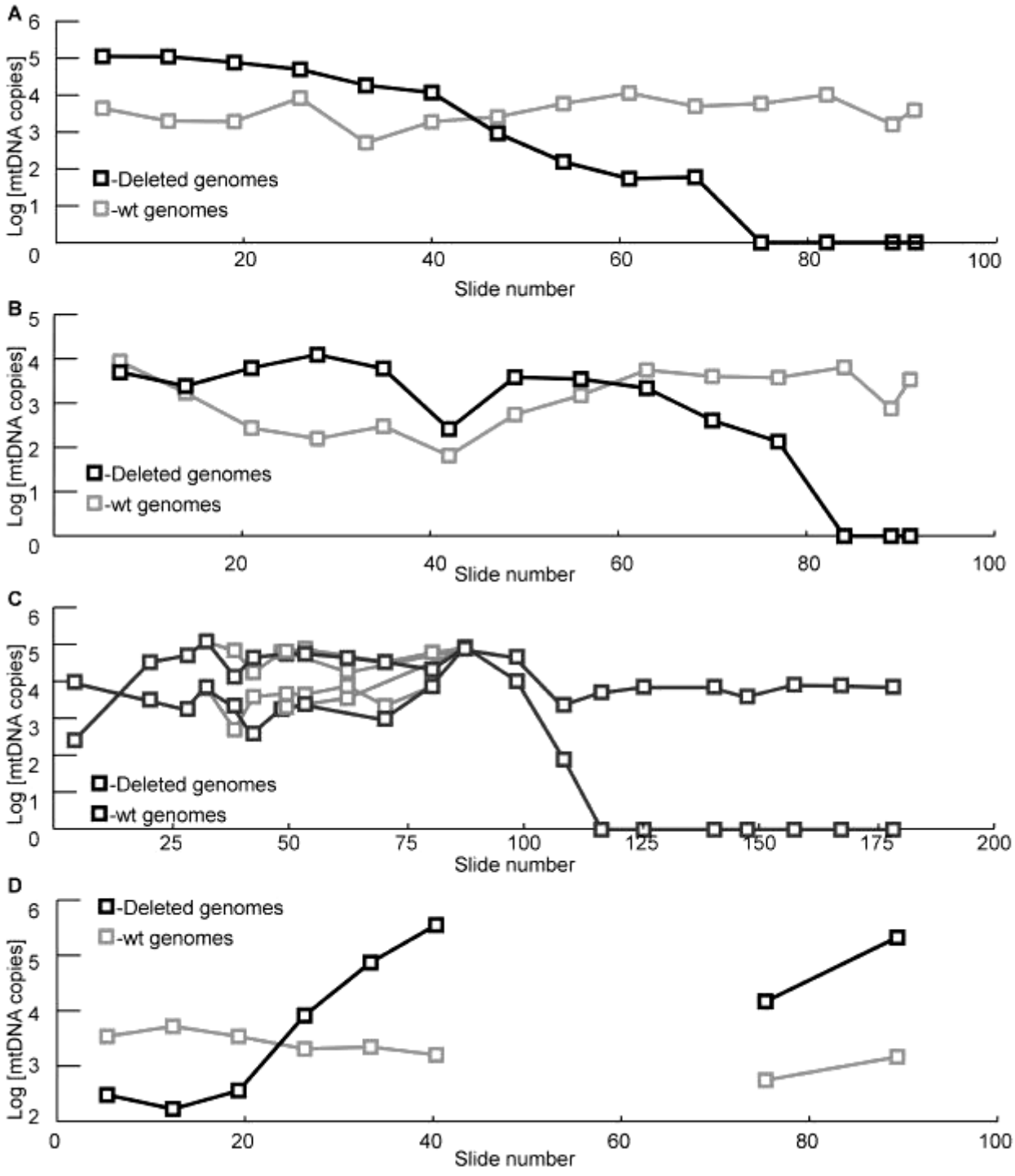

Figure 7. Absolute quantification of mitochondrial DNA (mtDNA) genomes. (**A**) Fiber 1; (**B**) fiber 2; (**C**) fiber 3; (**D**) fiber 4. Each branch of the split fiber is represented by a different line.

accumulate to cause ETS abnormal fibers. The localization of mtDNA deletion mutation breakpoints from ETS abnormal fibers to the major arc was previously attributed to the existence of a ''hot spot'' for mutation formation (34,39). The difference in deletion mutation patterns between tissue homogenates and single cells, however, suggests an alternative explanation: that the generation of mtDNA deletion mutants is random but that certain mutations, those producing small genomes (large deletions) while retaining both origins of replication, are more likely to accumulate to high intracellular abundance.

Many mechanisms have been proposed to explain the

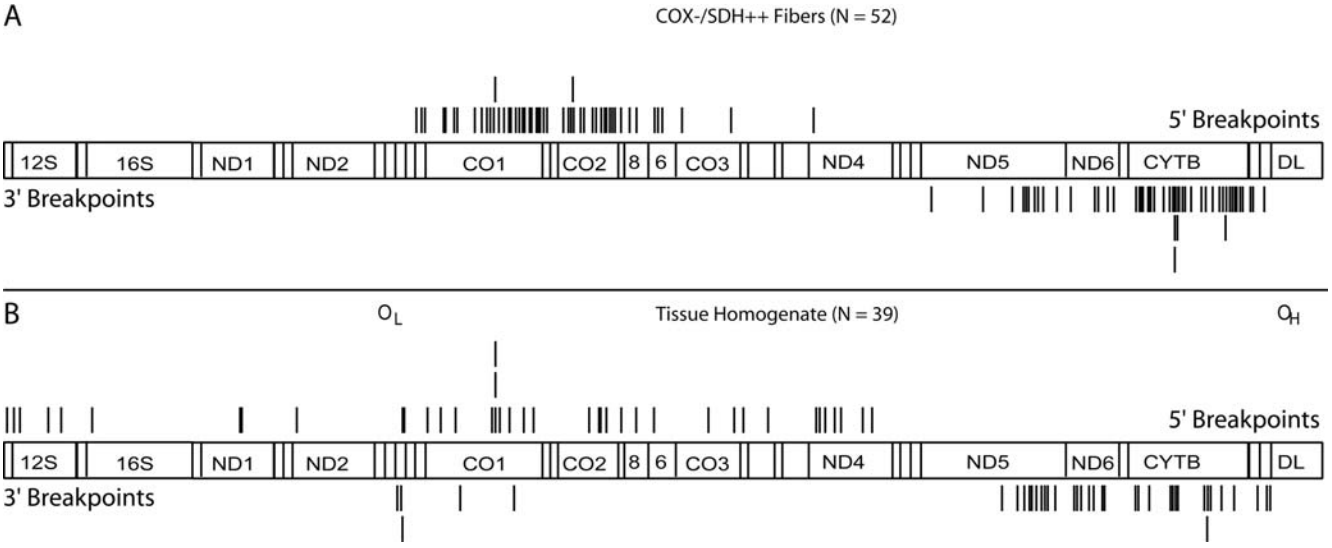

Figure 8. Distribution of the mitochondrial DNA (mtDNA) deletion breakpoints. *Top lines*: 5′ breakpoint; *bottom lines*: 3' breakpoint. O_L and O_H: Light-strand and heavy-strand origins of replication, respectively. (**A**) Deletion mutations from individual electron transport system abnormal fibers. Breakpoints occur within the major arc of the mitochondrial genome adjacent to the light-strand and heavy-strand origins of replication. (**B**) Deletion mutations from tissue homogenates. Breakpoints are scattered throughout the mitochondrial genome, occasionally removing the light-strand origin, but never removing the heavy-strand origin.

age-associated loss of muscle mass. Our molecular observations of the role of mtDNA deletion mutations in sarcopenia are consistent with the hypothesis that the intracellular accumulation of mtDNA deletion mutations causes mitochondrial dysfunction. The abrogation of mitochondrial and cellular processes induces morphological changes in the fiber such as splitting. The fiber atrophies and eventually ruptures. The somatic generation and subsequent intracellular accumulation of mtDNA deletion mutations contributes to the age-dependent loss of muscle fibers and sarcopenia.

Acknowledgments

This work was supported by National Institute on Aging Award R01 AG011604. We thank the National Institute of Environmental Health Sciences (NIEHS) Center for Molecular and Developmental Toxicology (ES 09090) for access to laser capture microdissection.

Correspondence

Address correspondence to Judd M. Aiken, PhD, University of Wisconsin, Department of Animal Health and Biomedical Sciences, 1656 Linden Dr., Madison, WI 53706. E-mail: aiken@svm.vetmed.wisc.edu

References

1. Harman D. The biologic clock: the mitochondria? *J Am Geriatr Soc*. 1972;20:145–147.
2. Miquel J, Economos AC, Fleming J, et al. Mitochondrial role in cell aging. *Exp Gerontol*. 1980;15:575–591.
3. Wallace DC. Mitochondrial diseases in man and mouse. *Science*. 1999;283(5407):1482–1488.
4. Trifunovic A, Wredenberg A, Falkenberg M, et al. Premature ageing in mice expressing defective mitochondrial DNA polymerase. *Nature*. 2004;429:417–423.
5. Kujoth GC, Hiona A, Pugh TD, et al. Mitochondrial DNA mutations, oxidative stress, and apoptosis in mammalian aging. *Science*. 2005;309:481–484.
6. Rosenberg IH. Sarcopenia: origins and clinical relevance. *J Nutr*. 1997;127:990S–991S.
7. Evans W. Functional and metabolic consequences of sarcopenia. *J Nutr*. 1997;127(5 Suppl):998S–1003S.
8. Lexell J, Taylor CC, Sjostrom M. What is the cause of the ageing atrophy? Total number, size and proportion of different fiber types studied in whole vastus lateralis muscle from 15- to 83-year old men. *J Neurol Sci*. 1988;84:275–294.
9. Sato T, Akatsuka H, Kito K, et al. Age changes in size and number of muscle fibers in human minor pectoral muscle. *Mech Ageing Dev*. 1984;28:99–109.
10. Wanagat J, Cao Z, Pathare P, et al. Mitochondrial DNA deletion mutations colocalize with segmental electron transport system abnormalities, muscle fiber atrophy, fiber splitting, and oxidative damage in sarcopenia. *FASEB J*. 2001;15:322–332.
11. McKiernan SH, Bua E, McGorray J, et al. Early-onset calorie restriction conserves fiber number in aging rat skeletal muscle. *FASEB J*. 2004; 18:580–581.
12. Cortopassi GA, Arnheim N. Detection of a specific mitochondrial DNA deletion in tissues of older humans. *Nucleic Acids Res*. 1990;18: 6927–6933.
13. Linnane AW, Baumer A, Maxwell RJ, et al. Mitochondrial gene mutation: the ageing process and degenerative diseases. *Biochem Int*. 1990;22:1067–1076.
14. Lee CM, Chung SS, Kaczkowski JM, Weindruch R, Aiken JM. Multiple mitochondrial DNA deletions associated with age in skeletal muscle of rhesus monkeys. *J Gerontol Biol Sci*. 1993;48:B201–B205.
15. Melov S, Hertz GZ, Stormo GD, et al. Detection of deletions in the mitochondrial genome of *Caenorhabditis elegans*. *Nucleic Acids Res*. 1994;22:1075–1078.
16. Chung SS, Weindruch R, Schwarze SR, et al. Multiple age-associated mitochondrial DNA deletions in skeletal muscle of mice. *Aging (Milano)*. 1994;6:193–200.
17. Simonetti S, Chen X, DiMauro S, et al. Accumulation of deletions in human mitochondrial DNA during normal aging: analysis by quantitative PCR. *Biochim Biophys Acta*. 1992;1180:113–122.
18. Edris W, Burgett B, Stine OC, Filburn CR. Detection and quantitation by competitive PCR of an age-associated increase in a 4.8 kb deletion in rat mitochondrial DNA. *Mutat Res*. 1994;316:69–78.
19. Schwarze SR, Lee CM, Chung SS, et al. High levels of mitochondrial DNA deletions in skeletal muscle of old rhesus monkeys. *Mech Ageing Dev*. 1995;83:91–101.

20. Mita S, Schmidt B, Schon EA, et al. Detection of ''deleted'' mitochondrial genomes in cytochrome-*c* oxidase-deficient muscle fibers of a patient with Kearns-Sayre syndrome. *Proc Natl Acad Sci U S A*. 1989;86:9509–9513.
21. Shoubridge EA, Karpati G, Hastings KEM. Deletion mutants are functionally dominant over wild-type mitochondrial genomes in skeletal muscle fiber segments in mitochondrial disease. *Cell*. 1990;62:43–49.
22. Oldfors A, Larsson NG, Holme E, et al. Mitochondrial DNA deletions and cytochrome *c* oxidase deficiency in muscle fibres. *J Neurol Sci*. 1992;110:169–177.
23. Moraes CT, Ricci E, Petruzzella V, et al. Molecular analysis of the muscle pathology associated with mitochondrial DNA deletions. *Nat Genet*. 1992;1:359–367.
24. Müller-Höcker J, Seibel P, Schneiderbanger K, et al. Different in situ hybridization patterns of mitochondrial DNA in cytochrome *c* oxidase-deficient extraocular muscle fibres in the elderly. *Virchows Arch A Pathol Anat Histopathol*. 1993;422:7–15.
25. Lee CM, Lopez ME, Weindruch R, et al. Association of age-related mitochondrial abnormalities with skeletal muscle fiber atrophy. *Free Radic Biol Med*. 1998;25:964–972.
26. Lopez ME, Van Zeeland NL, Dahl DB, et al. Cellular phenotypes of age-associated skeletal muscle mitochondrial abnormalities in rhesus monkeys. *Mutat Res*. 2000;452(1):123–138.
27. Holt IJ, Harding AE, Morgan-Hughes JA. Deletions of muscle mitochondrial DNA in patients with mitochondrial myopathies. *Nature*. 1988;331:717–719.
28. Wallace DC. Diseases of the mitochondrial DNA. *Annu Rev Biochem*. 1992;61:1175–1212.
29. DiMauro S. Mitochondrial diseases: clinical considerations. *Biofactors*. 1998;7:277–285.
30. Smeitink J, van den Heuvel L, DiMauro S. The genetics and pathology of oxidative phosphorylation. *Nat Rev Genet*. 2001;2:342–352.
31. Rossignol R, Faustin B, Rocher C, et al. Mitochondrial threshold effects. *Biochem J*. 2003;370(Pt 3):751–762.
32. Shoubridge EA. Mitochondrial DNA diseases: histological and cellular studies. *J Bioenerg Biomembr*. 1994;26:301–310.
33. Bua EA, McKiernan SH, Wanagat J, et al. Mitochondrial abnormalities are more frequent in muscles undergoing sarcopenia. *J Appl Physiol*. 2002;92:2617–2624.
34. Cao Z, Wanagat J, McKiernan SH, et al. Mitochondrial DNA deletion mutations are concomitant with ragged red regions of individual, aged muscle fibers: analysis by laser-capture microdissection. *Nucleic Acids Res*. 2001;29:4502–4508.
35. Hayashi J, Ohta S, Kikuchi A, et al. Introduction of disease-related mitochondrial DNA deletions into HeLa cells lacking mitochondrial DNA results in mitochondrial dysfunction. *Proc Natl Acad Sci U S A*. 1991;88:10614–10618.
36. He L, Chinnery PF, Durham SE, et al. Detection and quantification of mitochondrial DNA deletions in individual cells by real-time PCR. *Nucleic Acids Res*. 2002;30(14):e68.
37. Elson JL, Samuels DC, Turnbull DM, et al. Random intracellular drift explains the clonal expansion of mitochondrial DNA mutations with age. *Am J Hum Genet*. 2001;68:802–806.
38. de Grey ADNJ. A proposed refinement of the mitochondrial free radical theory of aging. *Bioessays*. 1997;19:161–167.
39. Gokey NG, Cao Z, Pak JW, et al. Molecular analyses of mtDNA deletion mutations in microdissected skeletal muscle fibers from aged rhesus monkeys. *Aging Cell*. 2004;3:319–326.

Received May 12, 2006
Accepted August 4, 2006
Decision Editor: Huber R. Warner, PhD